

A 1000fps High SNR Voltage-domain Global Shutter CMOS Image Sensor with Two-stage LOFIC for In-Situ Fluid Concentration Distribution Measurements

Tetsu Oikawa¹, Rihito Kuroda^{1,2}, Keigo Takahashi¹, Yoshinobu Shiba^{2,3}, Yasuyuki Fujihara¹, Hiroya Shike¹, Maasa Murata¹, Chia-Chi Kuo¹, Yhang Ricardo Sipaubá Carvalho da Silva¹, Tetsuya Goto², Tomoyuki Suwa², Tatsuo Morimoto², Yasuyuki Shirai², Masaaki Nagase³, Nobukazu Ikeda³, and Shigetoshi Sugawa²

¹ Graduate School of Engineering, Tohoku University,

6-6-11-811, Aza-Aoba, Aramaki, Aoba-ku, Sendai, Miyagi, Japan 980-8579

² New Industry Creation Hatchery Center, Tohoku University, ³ Fujikin Incorporated

TEL: +81-22-795-4833, Email addresses: tetsu.oikawa.r4@dc.tohoku.ac.jp, rihito.kuroda.e3@tohoku.ac.jp

ABSTRACT

This paper presents a prototype global shutter CMOS image sensor (CIS) with high signal-to-noise ratio (SNR) and 1000 fps performances for in-situ fluid concentration distribution measurements. The developed 22.4 μm pitch pixel consists of a high UV-light robustness UV-visible-NIR waveband pinned photodiode (PD), two-stage lateral overflow integration capacitor (LOFIC) for wide dynamic range and high SNR and voltage-domain memory bank for global shutter (GS), both formed by high density Si trench capacitors. The developed CIS exhibited 69.8 dB maximum SNR, 123 dB dynamic range and 1000 fps maximum frame rate, and successfully captured images of dynamic movement of NO_2 gas concentration distribution in the vacuum chamber.

INTRODUCTION

Practical realization of smart manufacturing, agriculture and healthcare are critical to improve the productivity and sustainability of our society. In these fields, next generation IoT technologies are needed that can visualize concentration distribution of dynamically moving gases and liquids by non-invasive/non-destructive manners. For example, real-time visualization of gas concentration distribution inside process chamber of semiconductor manufacturing equipment would greatly improve process condition optimization as well as process diagnosis. Several concentration measurement methods using light absorption have been utilized in high performance liquid chromatography with linear array sensor^[1], gas concentration sensor with a single photodiode^[2] and so on. As in the equation below, the use of a strong light source and a sensor with a high full well capacity (FWC) can improve the SNR and enable high-precision measurements,

$$\text{SNR} = 20 \log_{10} \left(\frac{N_{\text{sig}}}{\sqrt{N_{\text{sig}}^2 + n_{\text{sys}}^2}} \right) \cong 20 \log_{10} \sqrt{N_{\text{sig}}} \quad (1)$$

where, N_{sig} is the number of signal electrons and n_{sys} is the input referred number of system noise electrons.

In conventional methods with linear array sensors or single point detectors, high FWC has been achieved by using a large PD or attaching a large capacitor to the PD. In order to acquire concentration distribution information with high accuracy by the absorption imaging, an image sensor with extremely high FWC pixels need to be developed. For instance, in order to achieve 70 dB SNR, an over 10Me^- FWC is needed.

There are several technologies to increase FWC in CMOS image sensors, such as stacking organic photoconductive film on reading circuit^[3], complementary carrier collection^[4] and lateral over flow integration capacitor (LOFIC)^[5,6] and so on. By using LOFIC, PD, FD and LOFIC can be optimized independently and due to its linear response it is suitable for high precision absorption imaging.

In addition to SNR, there are other requirements for absorption imaging. First, high speed and GS operation is desirable to capture fast-moving objects without distortion, such as gases in the semiconductor process chamber. When measuring the concentration of individual substances in a mixture gases or liquids, it is necessary to switch the light source with the appropriate wavelengths. Here the GS is advantageous to efficiently synchronize the exposure period and the light illumination timing. Thanks to the high density capacitor technologies reported recent years^[7-10], the noise performance of the voltage-domain GS CIS has been improved. Next, a wide spectral response covering UV, visible to NIR is also required to capture the light absorption of various materials.

A CIS for UV/visible/NIR absorption imaging that satisfies all of these requirements simultaneously has not yet been reported so far.

This paper presents a high-speed and high SNR voltage-domain global shutter CIS with two-stage LOFIC toward in-situ fluid concentration distribution measurements using absorption imaging.

DESIGN AND STRUCTURE OF DEVELOPED CMOS IMAGE SENSOR

Figs. 1 and 2 show the pixel layout and circuit diagrams of the developed CIS and pixel cross-section, respectively. It consists of a high UV-light robustness UV-visible-NIR waveband pinned PD with high concentration p^+ layer with steep dopant profile, two-stage LOFIC and voltage-domain memory bank with six S/H capacitors. High density Si trench capacitors were employed for LOFIC1 (71.4 fF), LOFIC2 (2.59 pF) and the memory bank (214.2 fF each) that consist of 1, 37 and 3 units of capacitor cells, respectively. Here the LOFIC capacitance values were designed to achieve 70 dB maximum SNR and approximately 30 dB SNR at the signal switching points. Also, the capacitance of the memory bank was designed to sufficiently reduce thermal noise. These trench capacitors were surrounded by a deep p-well to prevent a leakage between the PD and the inversion layer of trench capacitors. The highly reliable SiO_2 dielectric was employed to achieve low leakage.

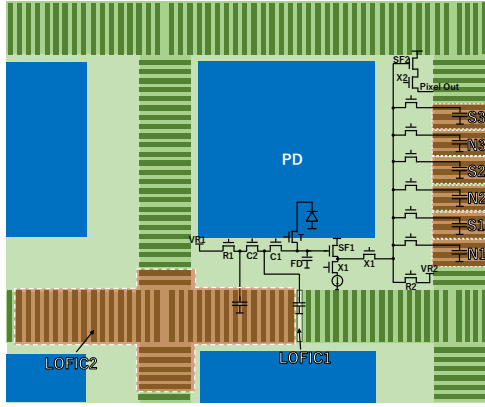


Fig. 1 Pixel layout and circuit diagrams of the developed CIS.

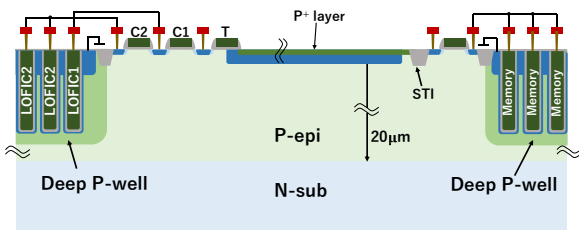


Fig. 2 Pixel cross section.

In addition, symmetrical and periodic arrangement of the capacitors reduces variation in optical and electrical characteristics. Recently a GS CIS for soft X-ray detector with two-stage LOFIC and memory bank was reported to be useful for wide dynamic range soft X-ray imaging^[11].

The gate sizes of the drive transistors for SF1 and SF2 and as well as the current sources were designed to enable 1000 fps operation.

Fig. 3 shows the circuit block diagram of developed CIS. It consists of pixel array, analog memory for pixel output, vertical and horizontal shift registers for signal readout and output buffers. The three differential pairs of high sensitivity, high saturation and the highest saturation signals are readout. The multiplexer between the GS operation mode and the row-by-row readout operation mode by Φ_{Read} . The HSR operates at 40 MHz for 1000 fps operation.

Fig. 4 shows the potential diagram and Figs. 5 and 6 show the GS and readout operation timing diagrams, respectively. In the GS operation, Φ_{Read} is set to low. Under a high illumination condition, photoelectrons overflow from the PD are accumulated in LOFIC1 and 2 (t_1). A reference signal for the high sensitivity S1 signal is readout by SF1 and stored in N1 memory (t_2). Photoelectrons in the PD are transferred to FD (t_3). A high sensitivity S1 signal is readout at FD (t_4), a high saturation S2 signal is readout at FD + LOFIC1 (t_5) and the highest S3 signal is read out at FD + LOFIC1 + LOFIC2 (t_6) and they are stored in the S1, S2 and S3 memories respectively. Then, PD are reset by R1 and reset signal for S3 is read out at FD + LOFIC1 + LOFIC2 (t_7) and reset signal for S2 is read out at FD + LOFIC1 (t_8) and they are stored in the N3 and N2 memories respectively. After all signals are readout, Φ_{Read} switches to high, and the readout operation and the integration time for the

next frame start. The signal of the row selected by the VSR is output to the column analog memories via the vertical signal line, and readout by the HSR to the horizontal signal line sequentially.

Fig. 7 shows the micrograph of the developed chip. The developed CIS was fabricated using a 0.18 μm 1-poly-Si 5-Metal CMOS image sensor process technology with pinned PD. The power supply voltage is 3.3 V and the die size is 4.8 $\text{mm}^{\text{H}} \times 4.8 \text{mm}^{\text{V}}$. The pixel size and the number of the effective pixels are 22.4 $\mu\text{m}^{\text{H}} \times 22.4 \mu\text{m}^{\text{V}}$ and 140^H \times 140^V, respectively.

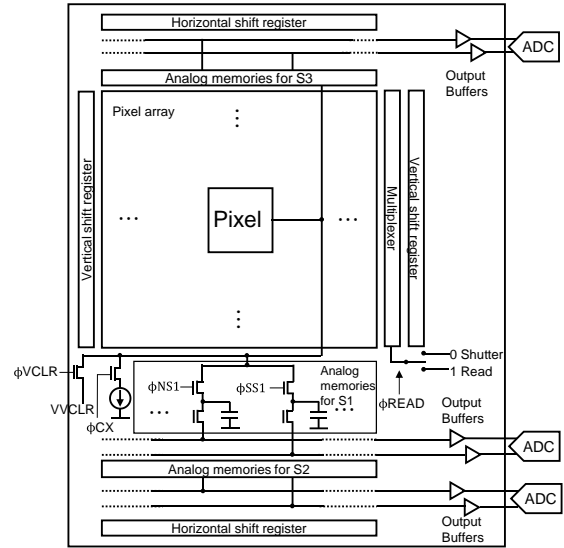


Fig. 3 Circuit block diagram.

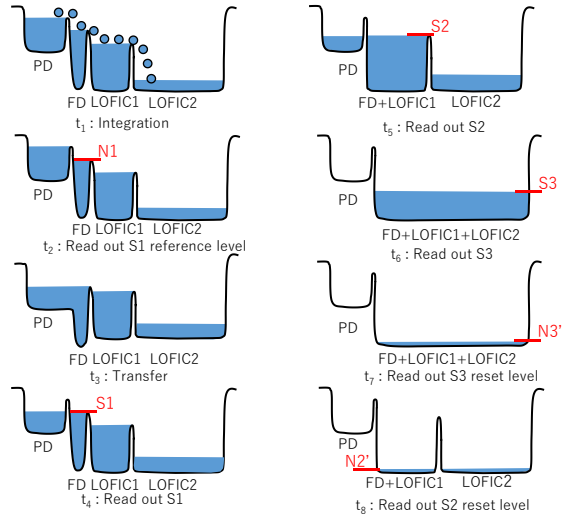


Fig. 4 Potential diagrams of two-stage LOFIC under high illumination.

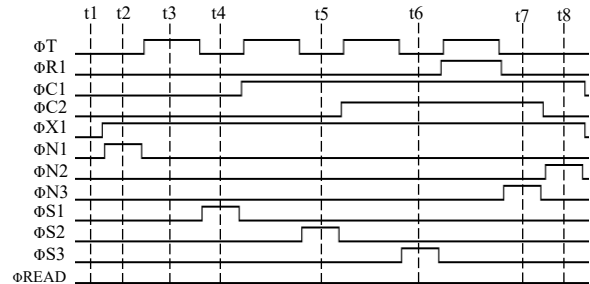


Fig. 5 Global shutter operation timing diagram.

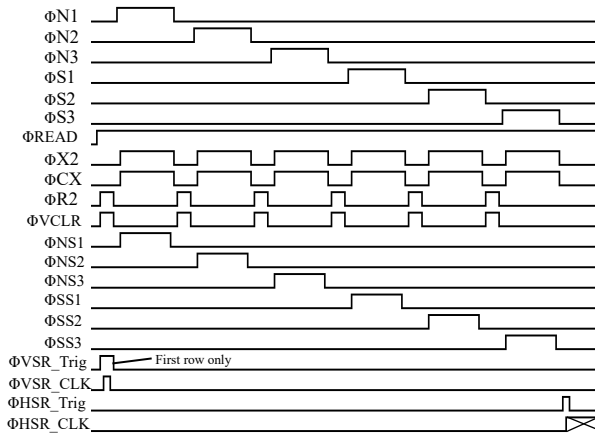


Fig. 6 Readout operation timing diagram.

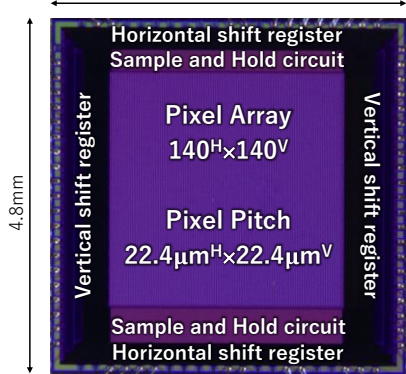


Fig. 7 Micrograph of the developed chip.

MEASUREMENT RESULTS

Figs. 8 and 9 show the measured photoelectric conversion and SNR characteristics. A green LED was used as the light source, and the integration times for S1, S2 and S3 signal were 1 ms, 4 ms and 21 ms, respectively. A 123 dB wide dynamic range was obtained under a single exposure by GS. The FWC of S1, S2 and S3 were $14.7ke^-$, $757ke^-$ and $27.8Me^-$ respectively. The maximum SNR of 69.7 dB was obtained for S3 signal. The high SNR is critically important for the high precision absorption imaging to detect sub-ppm order of fluid concentration. By always turning on the transfer gate and LOFIC switches to hold only the S3 signal, and by using the six S/H capacitors in the memory bank to perform correlated multiple sampling, the FWC can be further increased and the thermal noise and the low frequency noise of the first SF can be reduced, respectively to further improve the SNR.

Fig. 10 demonstrates the developed gas concentration distribution measurement system. In semiconductor manufacturing processes such as atomic layer deposition, chemical vapor deposition and etching, the control of the process gas concentration in the vacuum chamber is important for the atomic scale uniformity across the entire wafer substrate. The measurement system consists of the developed CIS, the vacuum chamber with six $150\text{ mm}^H \times 50\text{ mm}^V$ windows designed for the gas concentration visualization, and a 405 nm LED as light source. The wavelength corresponds to an absorption peak of NO_2 gas which is used as the measurement target. Here, NO_2 is often used for nitridation process for electron devices. By using three sets of sensors and light sources to capture images from three directions, this measurement

system is capable of measuring three-dimensional concentration distribution. As a preliminary experiment, two-dimensional concentration distribution of NO_2 gas in the vacuum chamber was visualized. Fig. 11 shows a calibration curve of absorbance obtained from the captured images for various gas flow ratio and pressure conditions. The absorbance in the calibration curve was calculated from the intensity of incident and transmitted light according to Lambert-Baer's law. The obtained results show a good linearity among various process conditions. Fig. 12 shows the captured images of NO_2 gas concentration in the vacuum chamber. The imaging focus was set to the center of the chamber, and the chamber pressure was 263Pa. Using a 25 mm F#4 lens, transient images were taken in an area of about $30\text{ mm}^H \times 40\text{ mm}^V$ when the total flow ratio of Ar and NO_2 was 1000 sccm and the flow ratio of NO_2 gas was changed from 0 to 10 percent. A dynamic movement of gas concentration distribution was successfully captured by 1000 fps GS absorption imaging as shown in Fig. 12. These images were obtained by coloring the absorbance. Here the incident light intensity distribution without absorption was captured when the NO_2 flow ratio was zero. The gas velocity estimated from the acquired images was approximately 7 m/s. The obtained in-situ and real-time measurement is useful to improve process condition as well as for the anomaly state detection of semiconductor equipment. Fig. 13 shows the relationship of maximum SNR and FWC, compared with other high saturation CIS for UV/visible/NIR imaging^[4,12-18]. The developed CIS achieved $27.8Me^-$ FWC and 69.7 dB maximum SNR under a single exposure GS operation. Table 1 summarizes the chip performances.

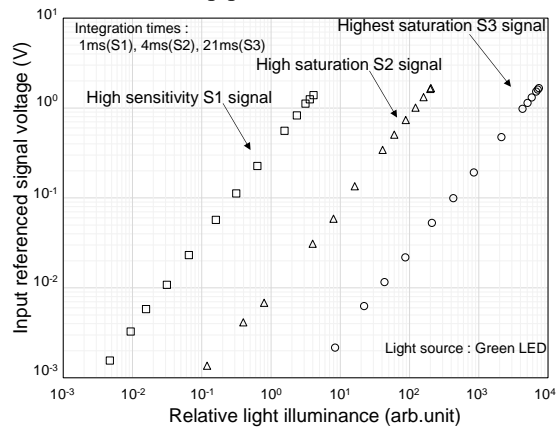


Fig. 8 Measured photoelectric conversion characteristics.

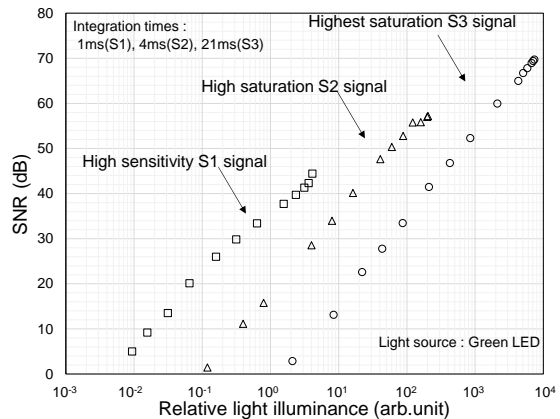


Fig. 9 Measured SNR characteristics.

CONCLUSION

A 22.4 μm pixel pitch global shutter CIS with two-stage LOFIC and voltage-domain memory bank was developed. Owing to its high SNR and high frame rate, the developed CIS successfully acquired images from the moving NO₂ gas in vacuum chamber with a linear calibration curve. The developed CIS is the key to the in-situ fluid concentration distribution measurements for various applications.

ACKNOWLEDGEMENT

This paper is based on results obtained from a project, JPNP19005, commissioned by the New Energy and Industrial Technology Development Organization (NEDO).

REFERENCES

- [1] V. Comet et al., Journal of Agricultural and Food Chemistry, Vol.54, No.3, pp.639-644, 2006.
 [2] H. Ishii et al., IEEE Sensors, pp.877-879, 2016.
 [3] M. Mori et al., Symp. VLSI Technology, Tech. Dig., pp.22-23, 2013.

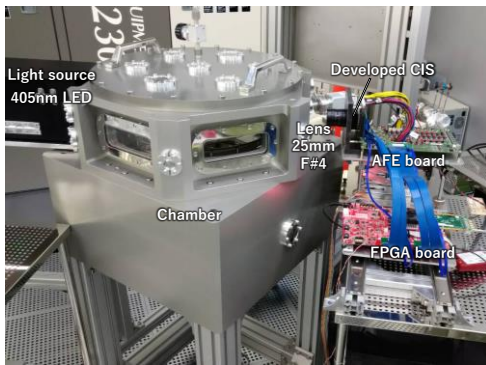


Fig. 10 Gas concentration distribution measurement system using absorption imaging for semiconductor manufacturing equipment.

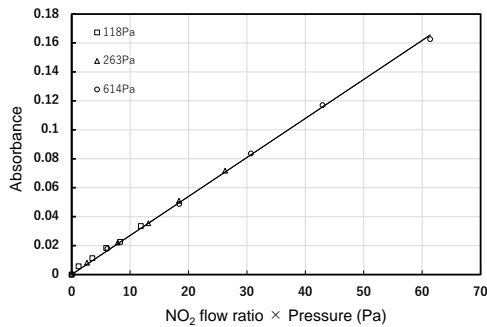


Fig. 11 Acquired calibration curve extracted from the obtained images. The product of gas flow ratio and pressure corresponds to the gas concentration.

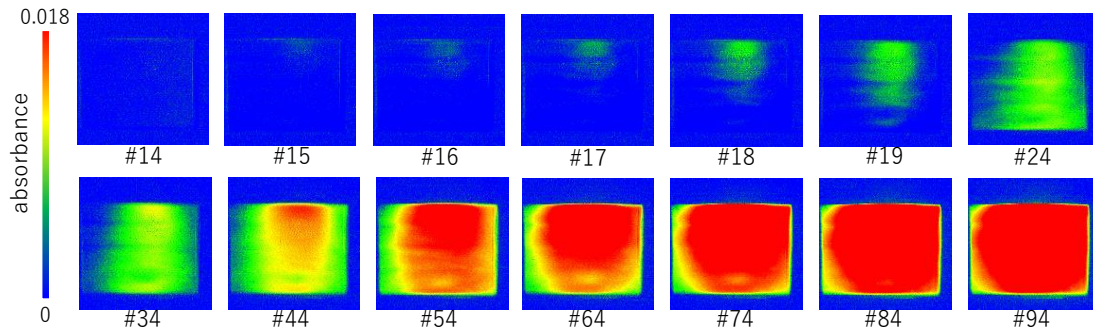


Fig. 12 Captured images of dynamic movement of NO₂ gas flow in the vacuum chamber at 1000fps. Flow ratio of NO₂ gas changed from 0 to 10% at 263Pa. (#corresponds to the frame number)

- [4] F. Lalanne et al., IISW2017, R30, 2017.
 [5] S.Sugawa, et al., ISSCC, Dig. Tech. Papers, pp.352-353, 2005.
 [6] Y. Fujihara et al., IEEE TED, Vol.68, No.1, pp.152-157, 2021.
 [7] M.Suzuki et al., IEDM, Tech. Dig., pp. 212-215, 2016.
 [8] G.Park et al., IEDM, Tech.Dig., pp.378-381, 2019.
 [9] J.Lee et al., ISSCC, Dig. Tech. Papers, pp.102-103, 2020.
 [10] M.Takase et al., Symp. VLSI Technology, Tech. Dig., pp.71-72, 2018.
 [11] H.Shike et al., IEEE TED, Vol.68, No.4, pp.2056-2063, 2021.
 [12] G. Meynants et al., IISW2017, R61, 2017.
 [13] N. Akahane et al., IEEE TED, Vol.56, pp.2429-2435, 2009.
 [14] M. Oh et al., IISW2019, R34, 2019.
 [15] M. Innocent et al., IISW 2019, P13, 2019.
 [16] X. Wang et al., IISW 2011, P36, 2011.
 [17] J. Solhusvik et al., IISW2017, R35, 2017.
 [18] S. Iida et al., IEDM, Tech. Dig., pp.221-224, 2018.

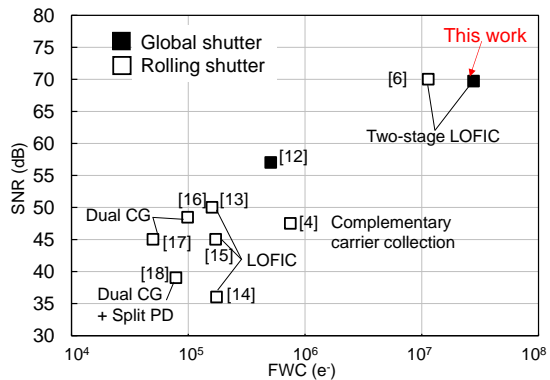


Fig. 13 Maximum SNR and FWC as benchmarking of developed CIS with other RS and GS CIS.

Table. 1 Performance summary.

Process technology	0.18 μm 1-poly-Si 5-Metal CMOS with pinned PD	
Power supply voltage	3.3V	
Die size	4.8mm ^H × 4.8mm ^V	
Pixel size	22.4 μm ^H × 22.4 μm ^V	
Fill factor	41%	
Electronic Shutter	Global shutter	
Maximum Frame rate	1,000fps@40MHz	
Conversion gain S1 signal	94.4 $\mu\text{V}/\text{e}^-$	
Conversion gain S2 signal	2.19 $\mu\text{V}/\text{e}^-$	
Conversion gain S3 signal	60.1nV/e ⁻	
FWC	High sensitivity S1	14.7ke ⁻
	High saturation S2	757ke ⁻
	Highest saturation S3	27.8Me ⁻
Maximum SNR	69.7dB	
Dynamic range	123dB	